machines

MDPI

Article

Network-Centric Formation Control and Ad Hoc Communication with Localisation Analysis in Multi-UAV Systems

Jack Devey [1], Palvir Singh Gill [1], George Allen [1], Essa Shahra [1] and Moad Idrissi [2,*]

[1] Faculty of Computing, Engineering and the Built Environment, Birmingham City University, Birmingham B4 7XG, UK; jack.devey@mail.bcu.ac.uk (J.D.); palvir.gill@mail.bcu.ac.uk (P.S.G.); george.allen@mail.bcu.ac.uk (G.A.); essa.shahra@bcu.ac.uk (E.S.)

[2] School of Computing and Data Science, Oryx Universal College | Liverpool John Moores University (OUC-LJMU), Doha P.O. Box 12253, Qatar

* Correspondence: moad.i@oryx.edu.qa

Abstract: In recent years, the cost-effectiveness and versatility of Unmanned Aerial Vehicles (UAVs) have led to their widespread adoption in both military and civilian applications, particularly for operations in remote or hazardous environments where human intervention is impractical. The use of multi-agent UAV systems has notably increased for complex tasks such as surveying and monitoring, driving extensive research and development in control, communication, and coordination technologies. Evaluating and analysing these systems under dynamic flight conditions present significant challenges. This paper introduces a mathematical model for leader–follower structured Quadrotor UAVs that encapsulates their dynamic behaviour, incorporating a novel multi-agent ad hoc coordination network simulated via COOJA. Simulation results with a pipeline surveillance case study demonstrate the efficacy of the coordination network and show that the system offers various improvements over contemporary pipeline surveillance approaches.

Keywords: UAV; multi-agent group; leader–follower; ad hoc network; simulation

Citation: Devey, J.; Gill, P.S.; Allen, G.; Shahra, E.; Idrissi, M. Network-Centric Formation Control and Ad Hoc Communication with Localisation Analysis in Multi-UAV Systems. *Machines* **2024**, *12*, 550. https://doi.org/10.3390/machines12080550

Academic Editors: Giuseppe Silano and Yahui Liu

Received: 28 June 2024
Revised: 2 August 2024
Accepted: 9 August 2024
Published: 13 August 2024

1. Introduction

1.1. Literature Review

Unmanned Aerial Vehicles (UAVs), more commonly known as drones, have garnered increased interests from both academia and industry due to notable advancements in sensor and computational capabilities, coupled with a reduction in their physical size. These factors make UAVs well suited for a diverse range of tasks [1]. Individual UAVs have proven themselves an invaluable aid to humanitarian and civilian life. Authors in [2] reason that recent advancements in both UAV and Internet of Things (IoT) technology have led to improved Precision Agriculture (PA) applications such as aerial crop monitoring or smart crop spraying. Similarly, in [3] drones are presented as a cost-effective alternative to manned aerial photogrammetry, or in [4] as a coastal engineering measurement tool. In [5], researchers discuss search and rescue applications, specifically a UAV's ability to quickly deploy communication networks in hostile environments such as those affected by nuclear or biological disasters.

Researchers foresee an increasing significance of drones in daily life. Drones will be a major delivery element by 2040, addressing a constant need for services in the industry [6]. Similarly, in [7], researchers discuss a blockchain-based healthcare system that relies on the use of UAVs for health data collection.

One of the major factors driving an increase in UAV research interest are developments in miniature UAVs. In [8], authors review the use of miniature UAVs in information acquisition, image processing, and crop management whilst also discussing limitations such as influence of wind or short battery life.

A multi-agent UAV group consisting of many UAVs working together in unison can overcome many shortcomings of independent flights as previously mentioned. These groups can also complete tasks faster and to a higher degree of accuracy. Works such as [9] explore and compare various communication techniques available for multiple UAVs. In [10], authors propose a UAV group comprising a singular leader and multiple followers tracking behind the leader using Wi-Fi signal strength. Alternatively, in [11,12], researchers discuss a resiliency method for swarms containing potentially malicious UAVs that share misleading coordination information in communication networks.

Groupings of UAVs are often regarded to be more cost-effective than traditional manned units. In [13,14], researchers also discover that the absence of a human pilot makes UAVs a more appealing option, as it eliminates the risk of fatalities in the event of a critical error. Additionally, UAVs can be perceived to decrease the number of manhours needed for maintenance due to their low complexity and fewer components.

Many recent multi-agent UAV studies have considered the implementation of various flocking algorithms for collective control and formation. In [15], researchers propose PASCAL, a novel curriculum-based multi-agent deep reinforcement learning approach for flocking of UAV swarms. The work's results suggest PASCAL is advantageous in learning efficiency and capable of generalising well for a variety of different swarm sizes. Additionally, authors of [16] propose a novel fractional-order flocking algorithm for effective use in large-scale UAV swarms that converges faster than traditional flocking algorithms.

Whilst flocking algorithms generalise well to large-scale swarms with potential applications in large-scale military surveillance or search and rescue (SAR) where the objective is to cover large areas quickly, they are not so well versed for refined low-altitude monitoring, where thorough and rigid formations are key.

One potential method to achieve rigid multi-agent group formations is the leader–follower approach. This consists of one UAV operating as a leader whilst other UAVs follow and replicate its movement at a pre-defined offset. In [17], researchers simulate a leader–follower structured group using a Sliding Mode Controller (SMC). Similarly, in [18], a backstepping-based leader–follower approach is simulated. Additionally, authors in [19] simulate a leader–follower collection along with a collision avoidance feature.

For UAV groups to function, networking is required to allow communication between drones. Works such as [20] discuss the five layers responsible for transmitting and receiving data: the application, transport, network, link, and physical layers. They play a critical part of moving information from one device or application to another.

There are two main protocols within the transport layer—TCP and UDP. In [21], authors discuss the minimal overhead required to use UDP and explain the increased delivery speeds whilst also highlighting reduced reliability. However, in [22], authors discuss TCP's error recovery mechanism and its higher degree of reliability at a cost of increased transmission time.

To orchestrate and organise network messages, an application layer technology must be used. Researchers in [23] explore the Hyper Text Transfer Protocol (HTTP), commonly used on the internet to serve content. Alternatively, authors in [24] discuss the Advanced Message Queuing Protocol (AMQP), an application-specific protocol for the RabbitMQ message broker ecosystem.

Message brokers are applications responsible for transferring volumes of data between services. Authors in [25] highlight the differences between RabbitMQ, which pushes data at a set rate to all receivers, and Kafka, which utilises a smart client system allowing for receivers to pull data at their own desired rates.

Ad hoc networking refers to the utilisation of wireless technologies to establish network connections between devices without the need for pre-existing infrastructure. In [26], authors discuss the lack of traditional infrastructure required to create an ad hoc network, but rather a device with an established connection to the internet acting as a gateway for devices in its local vicinity. Given the impracticality of traditional network infrastructure in airborne scenarios, the need for an ad hoc wireless network arises. In [27], authors discuss

a topology called Flying ad hoc networks (FANET). The gateway to the wider internet is the leader UAV, facilitating communications with the outside world for follower UAVs. Works such as [28] explain the use of dynamic routing or multi-hop protocols within ad hoc networks. Researchers in [29] highlight multi-hop protocols such as DV-hopping. These protocols are essential to ensuring data can be transmitted or received by nodes out of direct transmission range of the gateway.

1.2. Problem Formulation

Pipelines are essential for national energy security, providing a reliable source of oil transportation across countries and continents. Works such as [30] discuss the potential issues caused by pipeline deformation such as fatalities, economic impacts, and environmental pollution.

The Trans-Alaska Pipeline System (TAPS) located in Alaska (USA) is a pipeline that travels from Prudhoe Bay to Valdez Marina [31]. During its 800 mile span, the pipe travels through fault lines, mountain ranges, and rivers. It is constructed with over 42,000 double joints and over 66,000 field girth welds [32] (p. 36). Due to the scale of the pipeline and adverse terrain, regular inspections are imperative to ensure safe operations. The pipeline is of great importance to Alaska's economy, and downtime or loss of investment can have significant impacts.

Authors of [33] discuss a 7.9 magnitude earthquake that occurred 88 km west of the pipeline on 3 November 2002 . The pipeline remained intact; however, some supports were damaged, and it was shut down for 66 h and 33 min as a precaution [32] (p. 59). Should a similar scenario occur again, multi-agent UAV groups would provide an aerial surveying method to quickly discover and assess any potential damages, reducing overall downtime.

Significant sections of the pipeline are exposed, making them susceptible to numerous sabotages that often remain undetected for some time, leading to substantial oil spills. In February of 1978, an explosion caused a 1-inch hole in the pipeline, resulting in the leakage of approximately 16,000 barrels of oil before the pipeline was shut down [32] (p. 50). Similarly, in October of 2001, a bullet puncture caused a leak of 258,000 gallons and a shutdown of more than 60 h [32] (p. 58). In this scenario, UAV groupings could be used as a 24/7 surveillance measure to identify issues before they cause significant losses or be implemented to quickly discover oil spills in the surrounding area.

Previously, surveillance was carried out by manned aerial vehicles [34], until 2019, when a Beyond Visual Line of Sight (BVLOS) inspection of the pipeline was conducted using a UAV [35]. This process could be accelerated with the use of multi-agent UAV groups as they have the ability to execute tasks in parallel, drastically decreasing the time taken to complete the large-scale surveillance while simultaneously improving fault tolerance [36].

1.3. Contributions

In this study, a novel pipeline surveillance technique utilising a group of quadrotor UAVs for low-altitude monitoring is proposed. The primary objective of the proposed approach is to be more efficient than existing surveillance methods as previously deployed. The system facilitates round-the-clock data collection with each UAV accommodating a wide variety of sensor equipment for comprehensive data gathering and analysis across diverse environments.

In order to support this, a mathematical model of the multi-agent UAV's kinematics is derived. Additionally, a novel coordination network is proposed, suitable for supporting an implementation of the leader–follower structuring approach for real-world deployments. Both components are rigorously assessed in simulated environments with the goal of identifying the efficacy of these proposals.

The multi-agent group is structured using the leader–follower technique and consists of one leader being followed by three followers. Each follower is positioned to provide differing angles in visibility, allowing for a thorough and comprehensive assessment of the pipeline to be completed.

This work expands on previous studies such as [37] where researchers consider multi-agent UAV groupings as networked control systems (NCSs). However, in this study, UAV groups are considered as both kinematical systems and networking systems. By integrating these two perspectives, we aim to provide a more holistic and accurate assessment of the systems' efficacy in real-world scenarios. Specifically, our approach allows for the evaluation of both the physical dynamics and the communication efficiencies, offering insights into potential performance bottlenecks and optimisation opportunities when implementing networked control systems in UAV groups.

We also expand upon previous UAV-based pipeline inspection work by proposing a platform for multi-UAV deployments. For example, researchers in [38] propose a UAV-based inspection system for detecting loose bolts in pipeline structures, and our work proposes a system capable of distributing the inspection workload across many UAVs. This approach not only increases the inspection coverage and efficiency but also enables more rigorous investigations from various optical viewpoints. By leveraging multiple UAVs, our system can perform concurrent inspections, reducing downtime and enhancing the reliability of the inspection process.

Additionally, notable previous multi-agent UAV studies are presented for comparison with the work of this paper in Table 1. Of the Newton–Euler kinematical models selected for comparison, ours is the only study to assess our proposals against a rigorous case study, demonstrating the efficacy of our proposed systems in real-world environments. Additionally, the table shows we are one of few studies to consider both the necessary networking and kinematical aspects comprehensively. This dual consideration enhances the generalisability and robustness of our work, providing a significant contribution to the field by addressing the interdisciplinary challenges faced in real-world UAV deployments.

Table 1. Comparison of this work against previous multi-agent UAV research studies.

Ref	#UAVs	UAV Type/Model	Mass (kg)	Formation Control	Networking	Purpose
Ours	**4**	**Newton–Euler Kinematics**	**0.53**	**Leader–Follower**	✓	**Pipeline Surveillance**
[39]	5	Crazyflie 2.0	0.027	Rigid-Body	×	Indoor Flight Control
[18]	3	Newton–Euler Kinematics	1	Leader–Follower	×	Backstepping-based Control
[40]	6	Newton–Euler Kinematics	N/A *	Graph Theory	×	Time-varying Control
[17]	3	Newton–Quaternion Kinematics	0.26	Leader–Follower	×	Centralised Leader–Follower
[41]	10	N/A †	N/A †	Swarm Optimisation	×	PSO-based Control
[42]	10	N/A †	N/A †	Implicit Leaders	×	Implicit Leader Control
[43]	3	N/A †	N/A †	Reinforcement Learning	×	UAV Swarm Searching
[44]	N/A ‡	Newton–Euler Kinematics	N/A *	Leader–Follower	×	Heading Control System

* The work did not provide the chosen UAV mass constant. † The work maintains a high-level control perspective and no physical or kinematical UAV characteristics are considered. ‡ The work does not clearly state the number of UAVs used in the study.

To summarise, the major contributions of this work are presented below:

- A novel coordination network to facilitate the formation control of leader–follower structured multi-agent UAV operations.
- An improvement of existing pipeline surveillance techniques that utilises multiple UAVs for more comprehensive low-altitude data gathering, analysis, and differing perspectives of visibility.
- A rigorous simulation to assess the effects of the coordination network's transmission delays to ensure its negligible effect on overall tracking and mission performances.

1.4. Organisation

The remainder of this paper is organised as follows. Section 2 provides an introduction and explanation of the key technologies used in this work. Section 3 presents the

novel coordination network and improved surveillance technique with multi-agent UAVs. Section 4 demonstrates the effectiveness of the proposed technique with the simulation results. Finally, Section 5 concludes with a summary of the work and a discussion of potential areas for further research.

Figure 1 presents a flowchart that illustrates the main components of this article at each distinct section along with the flow of concepts throughout the paper.

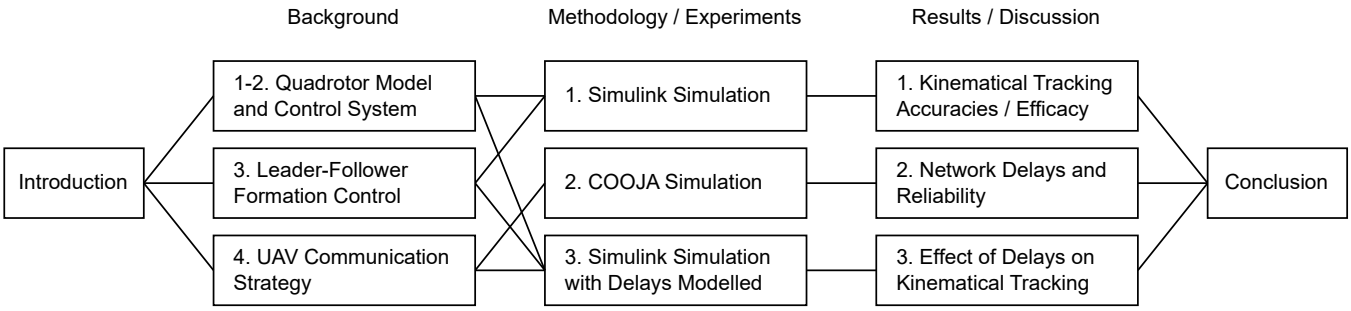

Figure 1. A flowchart illustrating the main components of this article at each distinct section with flow of concepts conducted in this study.

2. Background

2.1. Quadrotor Modelling

The quadrotors selected for this study are designed in a '+' configuration with four motors placed at 90° at an equal distance l to their centre of masses. To maintain stability, the limit for rolling and pitching is set to $\phi\,\mathrm{lim} = \theta\,\mathrm{lim} = 0.5$ rad.

The displacement of the quadrotor is measured with respect to the inertial frame of measurement [45], a fixed coordinate system based on the ground.

A quadrotor can typically be summarised with the use of 12 states, as shown in Equation (1).

$$\{x, \dot{x}, y, \dot{y}, z, \dot{z}, \phi, \dot{\phi}, \theta, \dot{\theta}, \psi, \dot{\psi}\} \tag{1}$$

where $\{x, \dot{x}, y, \dot{y}, z, \dot{z}\}$ is the position and linear velocities of the UAV and $\{\phi, \dot{\phi}, \theta, \dot{\theta}, \psi, \dot{\psi}\}$ are the rotations and angular velocities across the three rotational axes (rolling, pitching, and yawing, respectively).

The three main rotations are shown in the direct cosine matrix as below in Equation (2) [46], where s and c represent sine and cosine, respectively.

$$R = \begin{pmatrix} c_\psi c_\theta & c_\psi s_\theta s_\phi - c_\phi s_\psi & c_\phi s_\theta c_\psi + s_\psi s_\phi \\ c_\theta c_\psi & c_\psi s_\phi + s_\psi s_\theta s_\phi & s_\theta s_\psi c_\phi - c_\psi s_\phi \\ -s_\theta & c_\theta s_\phi & c_\theta c_\phi \end{pmatrix} \tag{2}$$

The input signals to adjust the position and rotation of the quadrotor can be written as U_1 for total thrust, U_2 for rolling, U_3 for pitching, and U_4 for yawing, in Equations (3)–(6), respectively, as in [47].

$$U_1 = b(\Omega_1^2 + \Omega_2^2 + \Omega_3^2 + \Omega_4^2) \tag{3}$$

$$U_2 = b(\Omega_2^2 - \Omega_4^2) \tag{4}$$

$$U_3 = b(\Omega_3^2 - \Omega_1^2) \tag{5}$$

$$U_4 = d(\Omega_1^2 - \Omega_2^2 + \Omega_3^2 - \Omega_4^2) \tag{6}$$

where b represents the thrust factor (6.317×10^{-4}), d represents the drag factor (1.61×10^{-4}) as calculated in [48], and Ω_i represents speed of the i th propeller (1–4).

As stated in [49], Equation (7), Ω_r offers the overall residual propeller speed which is used to calculate the gyroscopic effects during rotations.

$$\Omega_r = -\Omega_1 + \Omega_2 - \Omega_3 + \Omega_4 \tag{7}$$

The equations of motion for accelerations in the x, y and z directions and ϕ, θ and ψ rotations can be seen in Equations (8)–(13), respectively, as in [48]:

$$\ddot{x} = m^{-1}[\cos\phi \sin\theta \cos\psi + \sin\phi \sin\psi]U_1 \tag{8}$$

$$\ddot{y} = m^{-1}[\cos\phi \sin\theta \sin\psi - \sin\phi \cos\psi]U_1 \tag{9}$$

$$\ddot{z} = m^{-1}[\cos\phi \cos\theta]U_1 - g \tag{10}$$

$$\ddot{\phi} = I_x^{-1}[\dot{\theta}\dot{\psi}(I_z - I_y) - J_r\dot{\theta}\Omega + lU_2] \tag{11}$$

$$\ddot{\theta} = I_y^{-1}[\dot{\phi}\dot{\psi}(I_x - I_z) + J_r\dot{\phi}\Omega + lU_3] \tag{12}$$

$$\ddot{\psi} = I_z^{-1}[\dot{\phi}\dot{\theta}(I_y - I_x) + U_4] \tag{13}$$

where m is the total mass of a quadrotor, g is acceleration due to gravity, and l is the distance between the UAV's centre of mass and its motors.

2.2. Quadrotor Control

In order to sensibly control the UAV with respect to a coordinate system, a suitable control loop must be derived.

A Proportional-Integral-Derivative (PID) controller is employed to generate values for the U_1, U_2, U_3, and U_4 inputs according to the UAV's position across the x, y, z, and ψ dimensions, thus controlling the position and rotation of the quadrotor with respect to specified 'desired' values [50,51]. Equations (14)–(17) show the generation of control inputs for z, ϕ, θ and ψ, respectively.

$$U_{1c} = K_{pz}(z_d - z) + K_{iz}\int(z_d - z)dt + K_{dz}(\dot{z_d} - \dot{z}) \tag{14}$$

$$U_{2c} = K_{p\phi}(\phi_d - \phi) + K_{i\phi}\int(\phi_d - \phi)dt + K_{d\phi}(\dot{\phi_d} - \dot{\phi}) \tag{15}$$

$$U_{3c} = K_{p\theta}(\theta_d - \theta) + K_{i\theta}\int(\theta_d - \theta)dt + K_{d\theta}(\dot{\theta_d} - \dot{\theta}) \tag{16}$$

$$U_{4c} = K_{p\psi}(\psi_d - \psi) + K_{i\psi}\int(\psi_d - \psi)dt + K_{d\psi}(\dot{\psi_d} - \dot{\psi}) \tag{17}$$

To control the position of the quadrotor in the x and y directions, an outer-loop control system must first be introduced to generate ϕ_d and θ_d values from x_d and y_d. Works such as [46,52] often derive Equation (18) containing a mapping between attitude control inputs ϕ_d and θ_d and their respective acceleration control inputs of U_{cx} and U_{cy}.

$$\begin{bmatrix}\phi_d \\ \theta_d\end{bmatrix} = \frac{1}{g}\begin{bmatrix}\sin\psi & \cos\psi \\ \cos\psi & -\sin\psi\end{bmatrix}^{-1}\begin{bmatrix}U_{cx} \\ U_{cy}\end{bmatrix} \tag{18}$$

Further simplifying (18) by inverting the matrix (using its determinant $\sin^2\psi + \cos^2\psi$) yields Equation (19).

$$\begin{bmatrix}\phi_d \\ \theta_d\end{bmatrix} = \frac{1}{g(-\sin^2\psi - \cos^2\psi)}\begin{bmatrix}-\sin\psi & -\cos\psi \\ -\cos\psi & \sin\psi\end{bmatrix}\begin{bmatrix}U_{cx} \\ U_{cy}\end{bmatrix} \tag{19}$$

Using the Pythagoras rule for sine and cosine, $-\sin^2\psi - \cos^2\psi$ can be simplified to -1 and linearised into Equations (20) and (21) producing two independent sources of ϕ_d and θ_d, respectively.

$$\phi_d = \frac{1}{g}(U_{cx}\sin\psi + U_{cy}\cos\psi) \tag{20}$$

$$\theta_d = \frac{1}{g}(U_{cx}\cos\psi - U_{cy}\sin\psi) \tag{21}$$

Finally, the acceleration control inputs of U_{cx} and U_{cy} can be generated using Equations (22) and (23), which generate a control signal to reach desired x_d and y_d values.

$$U_{cx} = K_{px}(x_d - x) + K_{ix}\int(x_d - x)dt + K_{dx}(\dot{x_d} - \dot{x}) \tag{22}$$

$$U_{cy} = K_{py}(y_d - y) + K_{iy}\int(y_d - y)dt + K_{yx}(\dot{y_d} - \dot{y}) \tag{23}$$

Therefore, the full implementation of the quadrotor model can now be interfaced with using x_d, y_d, and z_d for influencing movement along the three respective axes or with ψ_d to influence yawing rotations.

2.3. Leader–Follower Structure

The leader–follower structuring approach consists of one UAV operating as a leader whilst other follower UAVs reproduce its movements at an additional pre-defined offset.

This approach is explained below using vector notation where $\hat{i}$ is a unit vector representing travel in the x direction, $\hat{j}$ is a unit vector representing travel in the y direction, and $\hat{k}$ is a unit vector representing travel in the z direction.

Vector $\vec{L}$ is composed of the current desired x, y, and z values of the leader quadrotor. These are represented as l_{dx}, l_{dy}, and l_{dz}, respectively in (24).

$$\vec{L} = l_{dx}\hat{i} + l_{dy}\hat{j} + l_{dz}\hat{k} \tag{24}$$

Vector $\vec{d_n}$ is composed of the displacement between the leader and follower n in all x, y, and z directions as in Equation (25).

$$\vec{d_n} = d_{nx}\hat{i} + d_{ny}\hat{j} + d_{nz}\hat{k} \tag{25}$$

Therefore, the emergence of an n-sized leader–follower formation in three dimensions can be represented in matrix form as in Equation (26).

$$\begin{bmatrix} \vec{d_1} \\ \vdots \\ \vec{d_n} \end{bmatrix} = \begin{bmatrix} d_{1x} & d_{1y} & d_{1z} \\ \vdots & \vdots & \vdots \\ d_{nx} & d_{ny} & d_{nz} \end{bmatrix} \begin{bmatrix} \hat{i} \\ \hat{j} \\ \hat{k} \end{bmatrix} \tag{26}$$

Equation (27) represents the position vector of follower n, derived from the addition of the leader's desired position $\vec{L}$ to the followers' unique displacement vector $\vec{d_n}$.

$$\vec{p_n} = \vec{L} + \vec{d_n} \tag{27}$$

Multiple followers can be implemented in various patterns as long as $\vec{d_n}$ is unique and nonzero across all followers as illustrated in Figure 2. Symmetrical shapes and patterns can be created as a result of negating components of $\vec{d_n}$.

At given intervals, $\vec{p_n}$ is computed and decomposed to form x_{nd}, y_{nd}, and z_{nd} desired values for each quadrotor's control loop to manage its own adjustments as shown in Equation (28).

$$\vec{p_n} = x_{nd}\hat{i} + y_{nd}\hat{j} + z_{nd}\hat{k} \tag{28}$$

2.4. Network and Communication Structure

Table 2 compares the use of the common network simulation software: COOJA (2.7), NS-2 (2.35) and Packet Tracer (8.2.2). COOJA is selected for this study as it provides the most realistic simulation platform for ad hoc IoT networks whilst also compiling the full ContikiOS for each device. Many projects have used COOJA to simulate ad hoc networks, such as [53], where both static and mobile networks were simulated for performance testing in COOJA, or in [54], where the performance of trilateration and centroid localisation

protocols was evaluated, or [55], where authors used COOJA for simulating intrusion detection systems.

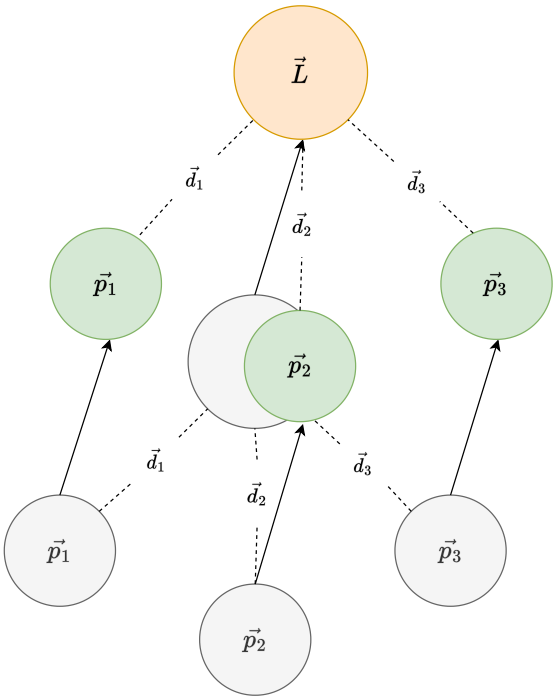

Figure 2. The proposed 4-drone grouping consisting of a leader (orange) and three follower drones $\vec{p}_n$ (green), including their previous positions before movement (grey).

Table 2. Comparison of the considered networking simulators.

Simulator	Description	Advantages	Disadvantages
COOJA	A ContikiOS simulator often used to simulate memory-constrained systems and low-power IoT devices.	Suitable for simulating low-powered devices [56] and simulations run on emulated hardware [57].	Minimal documentation available and complicated to use and develop with.
NS-2	An event-driven network simulator for simulation internet communication protocols.	Strong documentation and 3rd-party support with plugins [58].	Lack of a sensing model [58] and packet formats differ from Wireless Sensor Network (WSN) platforms [58].
Packet Tracer	A purpose-built network simulator and teaching tool developed for Cisco products [57].	Strong documentation with a focus on network design in the real world [57] and a user-friendly interface.	Not designed for IoT devices and simulations cannot translate into the real world easily.

The role of the ad hoc network is to share coordination information between UAV nodes in order to sustain an implementation of the leader–follower structuring approach. The system ensures that each of the follower UAVs are provided with the information necessary to uphold accurate formations during missions.

In the proposed network, an external control server is in constant communication with the leader UAV over an external wireless link such as radio, 4G, or 5G depending on regional connectivity. Over this connection, the control server periodically sends desired coordinates for the leader UAV to travel to. The coordinates sent from the control server feature on a pre-formulated mission plan or be recently generated for real-time operation. These coordinates are provided to the UAV's control system over a physical on-device connection to encourage the leader UAV to begin moving to the target coordinate.

Upon receiving new desired coordinates from the control server, the leader then derives individual coordinates to be sent to each of its followers as shown in Equation (27). Each follower then receives its unique coordinates from the leader and begins moving towards these points.

Algorithm 1 outlines the algorithmic steps followed by each node type.

Algorithm 1 The algorithmic steps of each node type featured in the coordination network.

procedure CONTROL SERVER(connection, interval)
  while true **do**
    if time % interval = 0 **then**
      $l_{dx} \Leftarrow$ Current desired x value for the leader
      $l_{dy} \Leftarrow$ Current desired y value for the leader
      $l_{dz} \Leftarrow$ Current desired z value for the leader
      Send (l_{dx}, l_{dy}, l_{dz}) to the leader over the connection
    end if
  end while
end procedure
procedure LEADER(connection, followers[], offsets[])
  while true **do**
    if (l_{dx}, l_{dy}, l_{dz}) received over the connection **then**
      for each index (i) in followers[] **do**
        $p_{idx} \Leftarrow l_{dx} +$ offsets$[i].x$
        $p_{idy} \Leftarrow l_{dy} +$ offsets$[i].y$
        $p_{idz} \Leftarrow l_{dz} +$ offsets$[i].z$
        Send $(p_{idx}, p_{idy}, p_{idz})$ to followers$[i]$ over the connection
      end for
      Move to (l_{dx}, l_{dy}, l_{dz})
    end if
  end while
end procedure
procedure FOLLOWER(connection)
  while true **do**
    if $(p_{idx}, p_{idy}, p_{idz})$ received over the connection **then**
      Move to $(p_{idx}, p_{idy}, p_{idz})$
    end if
  end while
end procedure

Additionally, Figure 3 shows a high-level diagram explaining the proposed network topology. Leader UAVs may also choose to transfer information back to the control server for processing or retention purposes such as video streams for remote viewing [59].

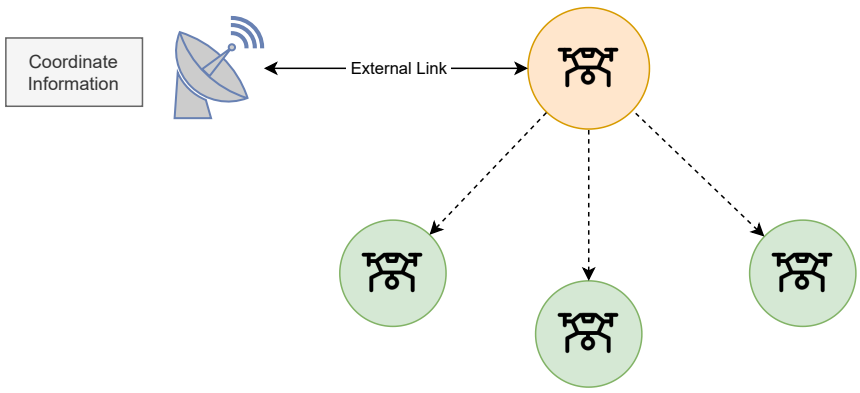

Figure 3. A high-level system diagram of the proposed network topology.

3. Methodology

To assess the efficacy of our system, two individual simulations commence. MATLAB/Simulink is used to simulate each UAV's kinematics to provide insight into the path-following ability of the UAV group. Alternatively, COOJA is used to investigate the accuracy and reliability of the coordination network in a separate test with a simulated topology analogous to the formation used in Simulink.

For further insight into the potential delays posed by networking-based coordination, the average time delays for each UAV to receive new coordination instructions are modelled in conjunction with their kinematics in Simulink in a final isolated experiment.

3.1. Simulink Simulation

During the group's simulation, each UAV travels along a pre-defined trajectory using coordinates approximated from a real section of the pipeline with Google Maps, as expressed in Figure 4. The route includes navigation around an expansion loop, a complex feature that repeats throughout the length of the real pipeline. During simulation, the path is assumed to stay at a constant measurement of 5 m in the z axis.

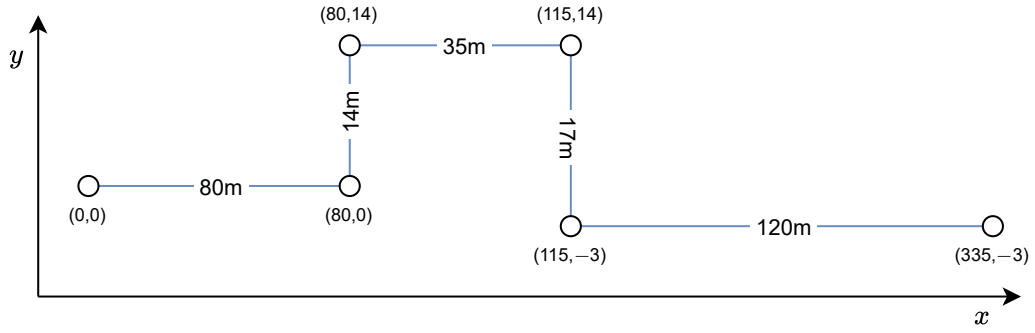

Figure 4. The chosen simulated path, an approximated short section of the Trans-Alaska Pipeline System.

As the majority of the pipeline consists of these repeated sections, if the UAVs demonstrate sufficient accuracy and control during navigation, it can be inferred that they hold the potential to track the longer distances in real-world scenarios.

The proposed formation for the simulation involves 2 followers positioned diagonally opposite to each other, each separated from the leader by 10 m, and 1 follower tracking 10 m directly behind. The formation can be represented in matrix form as in Equation (29).

$$\begin{bmatrix} \vec{d_1} \\ \vec{d_2} \\ \vec{d_3} \end{bmatrix} = \begin{bmatrix} -10 & 10 & 0 \\ -10 & 0 & 0 \\ -10 & -10 & 0 \end{bmatrix} \begin{bmatrix} \hat{i} \\ \hat{j} \\ \hat{k} \end{bmatrix} \tag{29}$$

When visualised in the 2D plane, this produces a triangular structure as illustrated in Figure 5. Followers 1 and 3 image each respective side of the pipeline, whilst Follower 2 focuses on the top view of the pipe. Therefore, all exposed surfaces of the pipeline can be sufficiently monitored.

The simulation commences in an environment without any external physical disturbances modelled. This provides a fair platform for evaluation of the leader–follower formation control scheme at a high level. For real-world deployments in outdoor environments, disturbance rejection techniques need to be implemented at each quadrotor's control layer [60,61]. The simulation also assumes that all UAVs in the grouping are homogeneous for simplicity.

The PID constants expressed in Table 3 and the physical parameters represented in Table 4 are employed for the duration of the simulation.

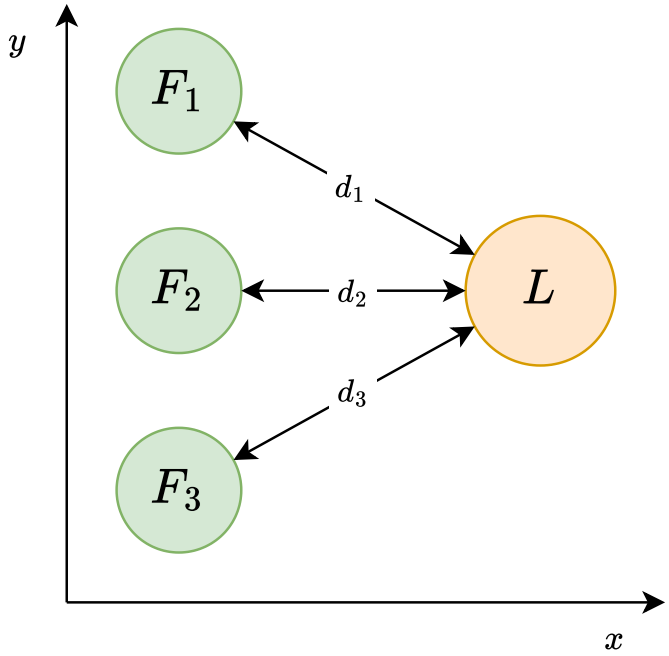

Figure 5. A 2D visualisation of the simulation formation as described in (29). The leader is represented in orange and each follower is in green.

Table 3. The chosen PID gain constants for the kinematics simulation in Simulink.

PID	K_p	K_i	K_d
x	3.9	0.001	4.3
y	3.9	0.001	4.3
z	10.1	0.01	7.5
ϕ	5.5	0.01	1.1
θ	5.5	0.01	1.1
ψ	4.2	0.01	0.8

Table 4. The chosen physical parameters for the kinematics simulation in Simulink.

Constant	Description	Value
g	Gravitational acceleration	9.81 m/s^2
l	Arm length	0.225 m
m	Quadrotor mass	0.53 kg
I_x	Inertia around x	5×10^{-3} kgm^2
I_y	Inertia around y	5×10^{-3} kgm^2
I_z	Inertia around z	8.9×10^{-3} kgm^2

At given time intervals during the simulation, the values of x_d and y_d of the Leader's control input values are updated to encourage the multi-agent network to move along the path. These coordinates and timings are shown in Table 5.

In a real-world deployment of this solution, these values originate from the control service and are transmitted to the leader via a network connection.

Table 5. The coordinates that form the desired positions (x_d, y_d, z_d) for the Leader UAV at each discrete time step.

Time	x_d	y_d	z_d
0 s	0	0	5
10 s	80	0	5
20 s	80	14	5
30 s	115	14	5
40 s	115	−3	5
50 s *	335	−3	5

* There is no 10 s time limit imposed on this stage as no more desired positions are to be sent.

3.2. Network Simulation

In COOJA, a similar formation as in Simulink is emulated, with the inclusion of the external controlling service. During the simulation, this service generates random coordinate pairs at 10 s intervals, allowing for the analysis of the time taken for information to travel through the network.

Figure 6 shows the network topology of the COOJA simulation. Motes are configured so that Mote 1 resembles the generator service, Mote 2 resembles the leader and Motes 3 to 5 resemble Followers 1 to 3, respectively.

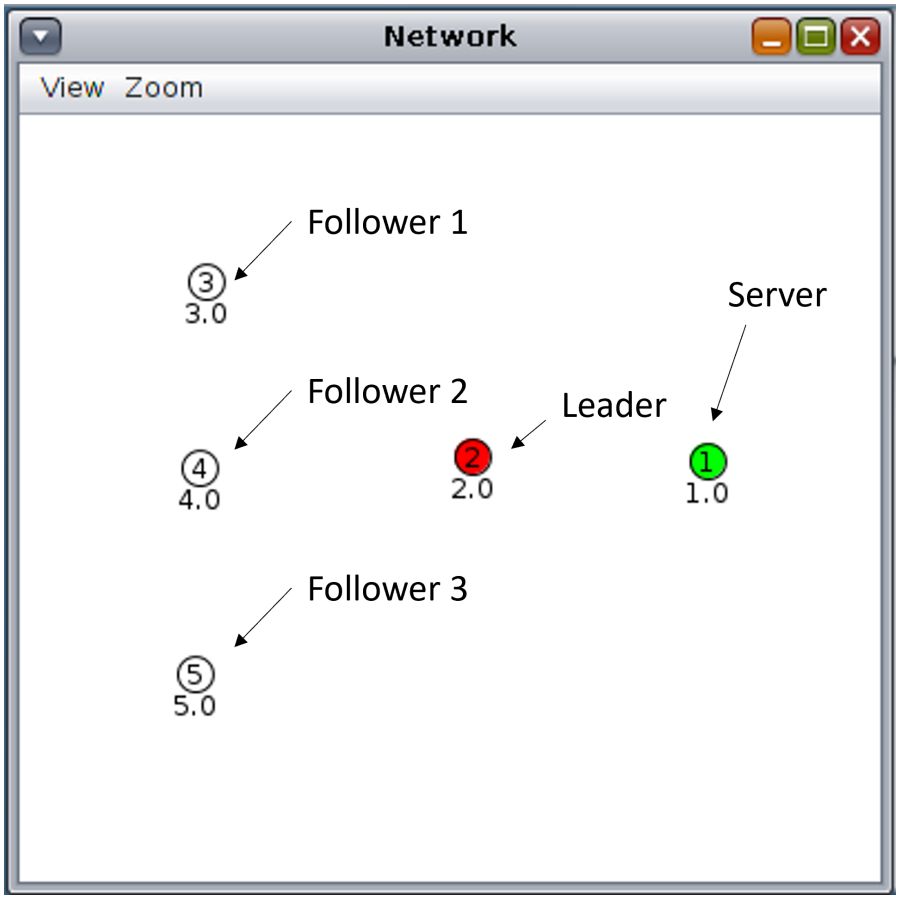

Figure 6. An annotated screenshot of the network topology of the COOJA simulation, showing the server, leader, and follower motes and their associated IP addresses.

Table 6 details the chosen COOJA environment parameters for the simulation. Zolertia Z1 motes are simulated as their low-power hardware [62] is suitable for real-world UAV-based IoT applications.

Table 6. The chosen simulation environment parameters as employed for the COOJA networking simulation.

Parameter	Value
Wireless Channel Mode	UDGM
Total Motes	5
Mote Type	Zolertia Z1
Transmission Range	50 m
Interference Range	100 m
Tx Ratio	100%
Rx Ratio	100%
Simulation Duration	60 min

The aim of the COOJA simulation is to provide insight into how accurately and timely our proposed coordination network functions over a rigorous experiment consisting of numerous randomly generated coordinate values.

4. Results

4.1. Simulink Simulation

A 3D plot of the positions of the group during simulation is depicted in Figure 7, suggesting a stable and accurate traversal of the target path. Follower UAVs remain at their designated distances, keeping a strong formation and a constant altitude of 5 m throughout the entire flight duration.

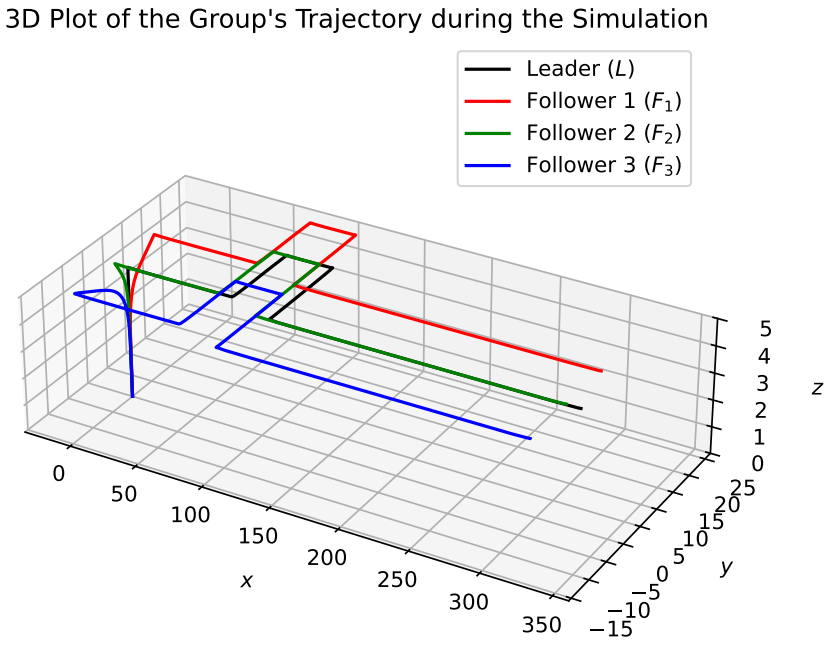

Figure 7. A 3D plot of the positions of the group during flight. The leader's path is black and the paths of followers 1–3 are red, green, and blue, respectively.

To quantify and measure the tracking performance of the group, the magnitude of error across all x, y, and z dimensions can be expressed by (30).

$$e(t) = \sqrt{(x_d(t) - x(t))^2 + (y_d(t) - y(t))^2 + (z_d(t) - z(t))^2} \tag{30}$$

where $e(t)$ defines the current positional error with respect to time t, $x_d(t)$ is the current desired position in x at time t, and $x(t)$ is the current actual position in x at time t.

A plot of the overall error can be seen in Figure 8, illustrating the group's accurate and performant trajectory tracking capabilities. At 10 s intervals, immediate vertical spikes are seen as each quadrotor's desired variables are updated by the new coordinates. Over the next few seconds, the error value is gradually reduced as the UAV begins to move towards its goal and its PID controllers aim to reduce their steady-state errors. All UAVs begin with various error distances and gather to form a single smooth line, indicating an accurate formation for the remainder of the simulation duration.

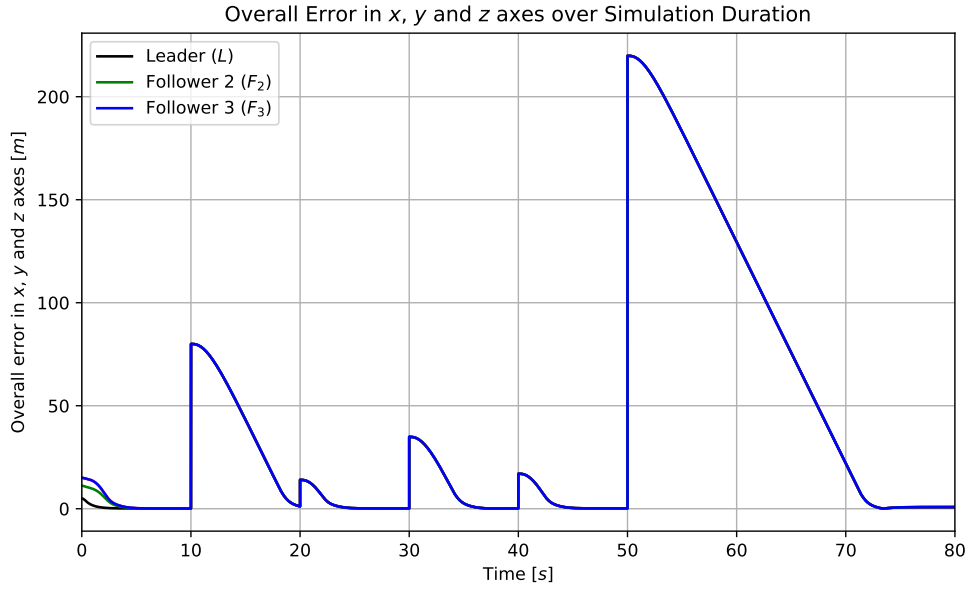

Figure 8. A plot of the overall error, showing the combined accuracy of the UAVs when traversing the trajectory. Follower 1 and follower 3's signals are identical so only follower 3's line is visible in the plot.

These results show the UAVs possess exemplary pipeline traversal abilities in the simulation environment. Translating to real-world applications, this suggests the system's potential for high accuracy and reliability in real-time monitoring and inspection tasks. The UAVs could therefore effectively track pipelines for surveillance and health checks, identifying issues such as leaks or structural anomalies. High accuracy in the simulation indicates the UAVs' capability to perform precise and thorough assessments of the pipeline.

Figures 9 and 10 show the group's displacements in the x and y directions, respectively, over the course of the simulation. All UAVs are able to maintain their desired distances between each other during the simulation, suggesting a high level of tracking accuracy across both dimensions. This highlights the system's robust coordination abilities, and for real-world deployments ensures that individual UAVs are able to consistently keep focus on their assigned portion of the target pipeline. This ensures that the pipeline surveillance objective is completed thoroughly and reliably.

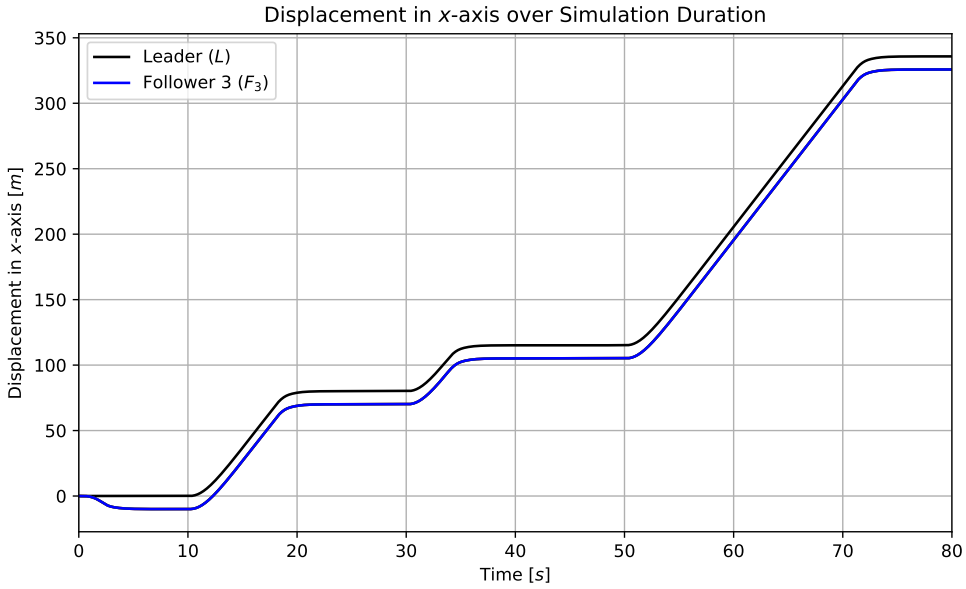

Figure 9. A plot of the displacement in the x-axis over the simulation time for all 4 UAVs. The leader is consistently ahead of each of the followers in the x-axis due to the formation utilised in the simulations. All follower signals are identical in the x-axis so only follower 3's signal is visible in the plot.

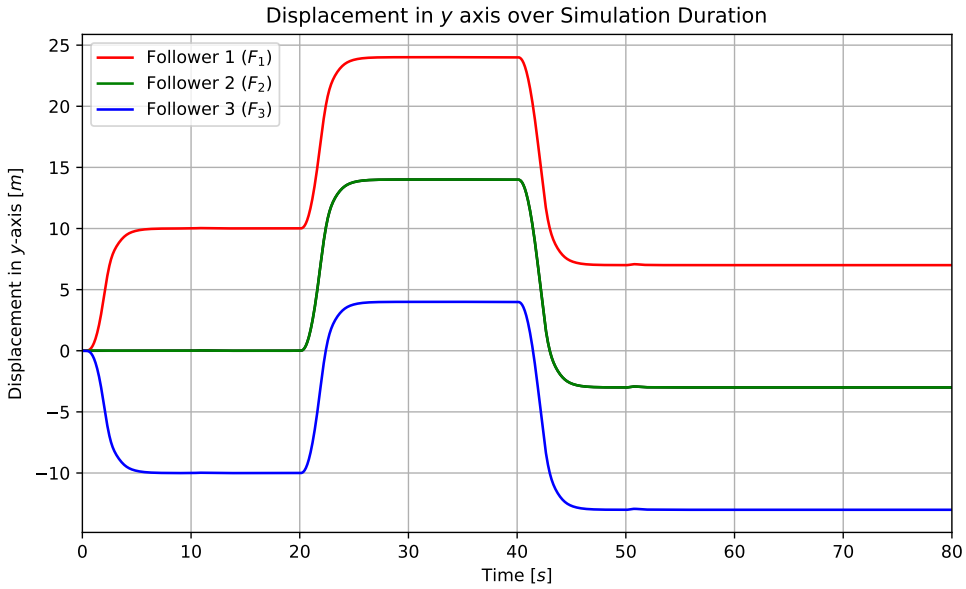

Figure 10. A plot of the displacement in the y-axis over the simulation time for all 4 UAVs. Followers 1 and 3 have unique y positions at all times due to the formation used in the simulations. Follower 2 has an identical position to the leader in the y-axis and therefore the leader's signal is not visible in the plot.

Finally, Figures 11 and 12 show the group's roll and pitch rotations during simulation. With the rotational limits of $+/-$ 0.5 rad imposed to ensure stability, all quadrotors are seen to make unified accurate and precise rotations during their movements in the x and y directions. This suggests each UAV is able to complete its mission in a steady and elegant manner, further confirming the efficacy and capability of real-world deployment.

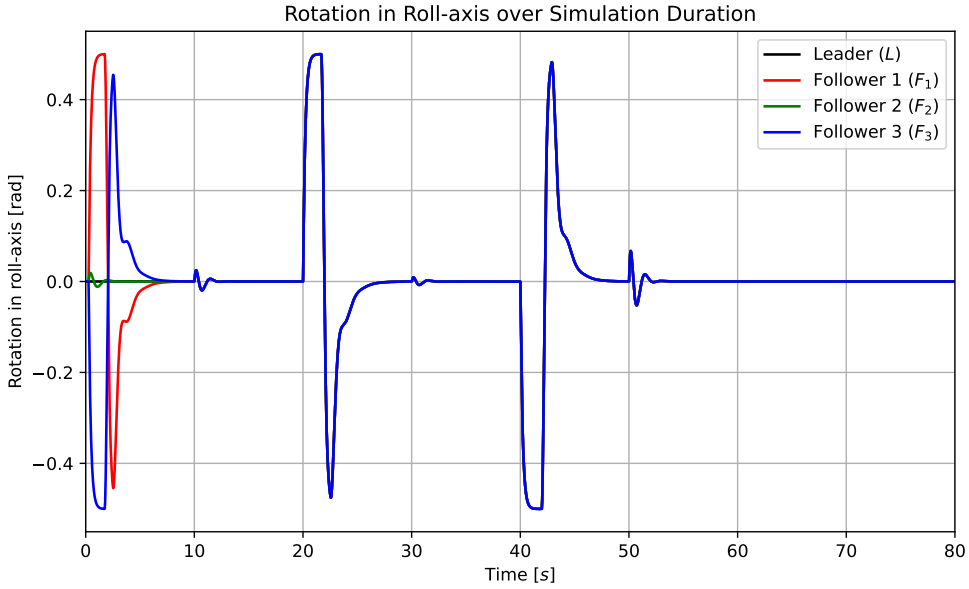

Figure 11. A plot of the rotation in the roll-axis over the simulation time for all 4 UAVs.

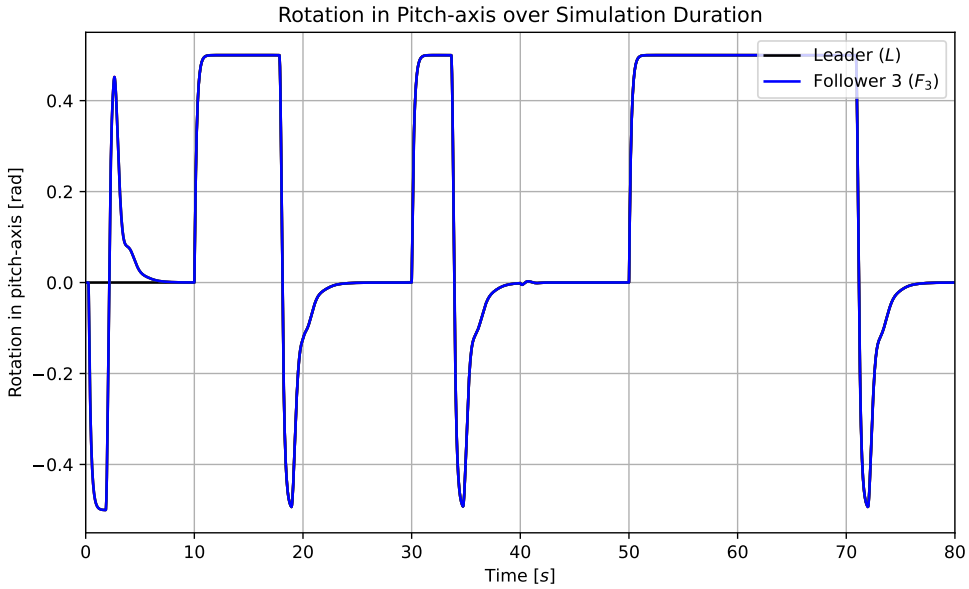

Figure 12. A plot of the rotation in the pitch-axis over the simulation time for all 4 UAVs. The followers rotate in unison leading to only follower 3's line being visible in the figure.

The simulation results depict the multi-agent UAV group's advanced capabilities in maintaining coordinated movements and stability. They demonstrate not only the precision required for effective pipeline surveillance but also the synchronisation necessary for collective task execution such as photogrammetry.

4.2. Network Simulation

An extract of the output logs as generated by the simulated Z1 motes during the simulation duration is shown in Figure 13. It can be observed that at $t \approx 59{:}41$, a dropped packet occurred, resulting in follower 3 (ID 5) not receiving its new coordinates.

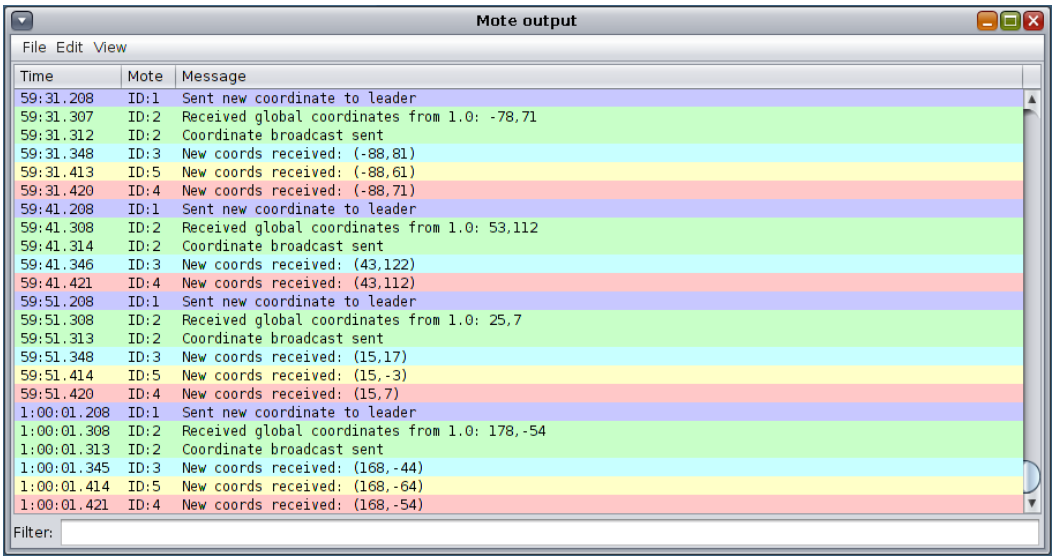

Figure 13. A screenshot of the output from COOJA during the simulation period, with the occurrence of a dropped packet visible at $t \approx 59{:}41$.

This accurately depicts one of the downfalls of the proposed coordination network as no packet re-delivery mechanism is available to address dropped packets. For real-world implementations, this could cause significant issues in UAV collaboration and communication as potentially some nodes would not receive new task instructions. Although missed packets are seen to be rare events, only 29 were experienced across all nodes out of the 1042 total packets sent. This approximates to an impressive failure rate of only 2.5%.

Due to the potentially disastrous effects of this occurring, even though there is a low likelihood, real-world deployments of this technology should implement a fault-tolerant protocol as in [63].

The average time taken for new coordinates to be acknowledged by each of the followers can be seen in Figure 14. There is a perceived average difference of 77 ms between the fastest receiver (Follower 1) and the slowest (Follower 2).

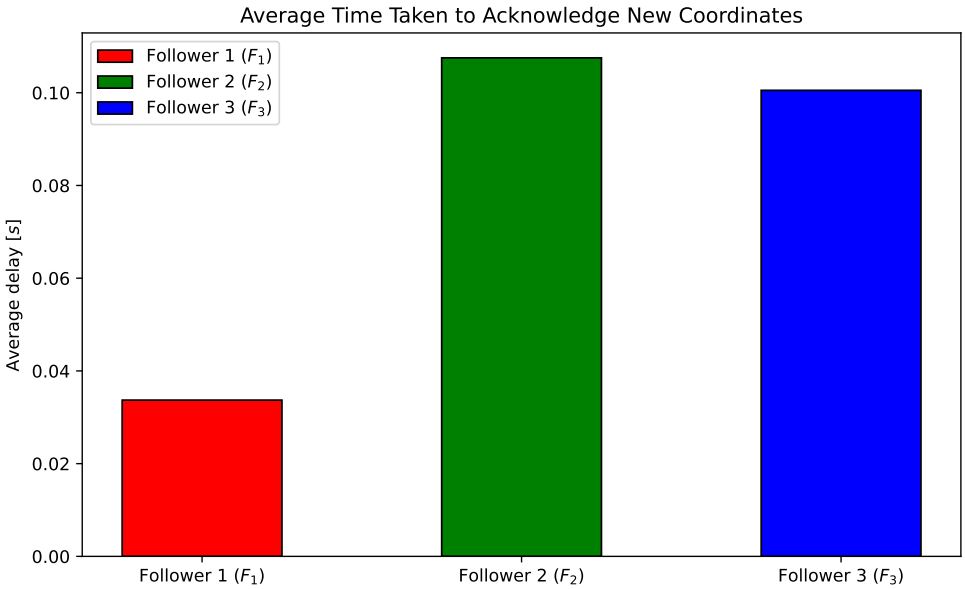

Figure 14. A bar chart showing the average time taken for each follower to receive a packet from the leader.

The differences in acknowledgement times across the three followers are attributed to the signal interference of the simulated environment coupled with the low-power simulated node hardware. Sending multiple messages at once would increase network traffic and therefore the processing load experienced by each of the follower nodes. This would decrease the responsibility and reactivity of each of the followers, explaining the sharp increase in acknowledgement times for followers 2 and 3.

Whilst even the slowest acknowledgement time is no major cause for concern, for real-world deployments of this technology, the capability of the hardware used for each network device must be carefully considered and assessed in order to ensure optimal performances.

4.3. Delay Analysis

By incorporating the average delays for each UAV from the COOJA network simulation into the Simulink model, a more rigorous and realistic evaluation of the overall effectiveness of the proposed approach can be performed.

Figure 15 shows a plot of the overall error, similar to Figure 8, but with the average delays for each UAV modelled. This suggests that the delays introduced during transmission of the coordinate data have negligible effects over the general accuracy and tracking abilities of the group. An enlarged portion of the graph at around 10 s illustrates the minimal disparity between each UAV receiving new coordinate information. With the leader (black) moving immediately, the followers receive the instructions within the same time frames as visible in Figure 13.

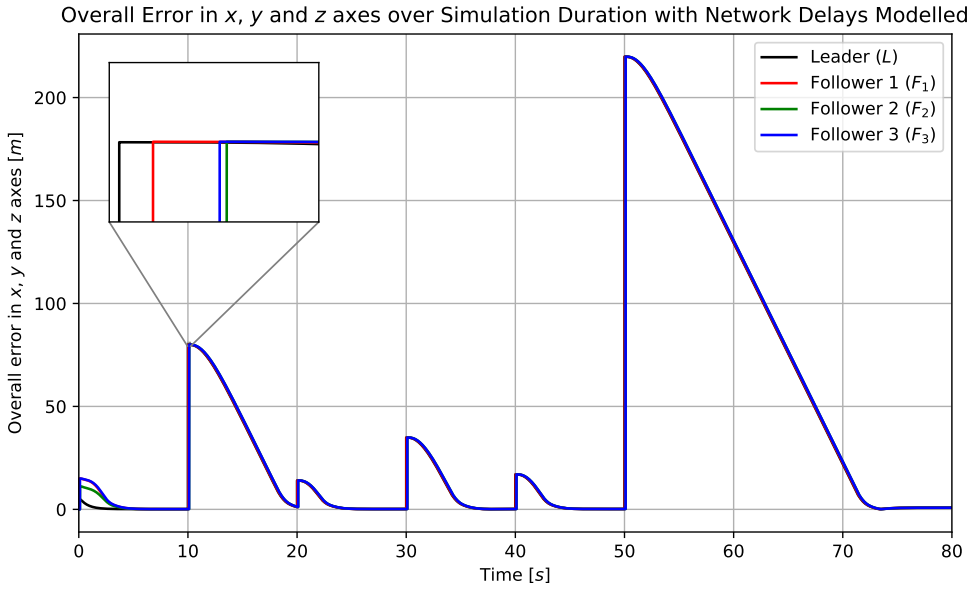

Figure 15. A plot of the overall error, showing the accuracy of the UAVs whilst traversing the trajectory is not impacted with the average transmission delays modelled. A further zoomed portion around 10 s shows the negligible effects of the delay.

The plot shown in Figure 15 is almost identical to the plot shown in Figure 8, which asserts that the delays posed by the networking coordination system have no overall effect on the UAVs' tracking abilities. All UAVs continue to collectively track the simulated pipeline with efficient and refined movements. This translates to an effective pipeline surveillance system should this be deployed to real-world environments.

5. Conclusions

In this paper, a novel pipeline surveillance method was proposed that utilises multiple UAVs structured in a leader–follower formation for improved efficiencies over existing single-UAV operations. The proposed system aims to revolutionise pipeline surveillance

approaches to provide a platform for the introduction of round-the-clock data collection with comprehensive sensor equipment.

A rigorous simulation of the multi-agent group's kinematics was executed using Simulink. A group of four UAVs traversed over a simulated portion of the Trans-Alaska Pipeline System, arranged in a formation to provide each with a unique perspective on external faces of the pipeline. Analysis of the extracted results suggest the UAVs possess exemplary tracking abilities, with each individual UAV rigidly keeping to its desired position within the formation during movement.

Further analysis of the kinematical simulation's results infer the group collectively makes elegant and effective movements, suggesting the UAVs offer a reliable and stable platform for data collection devices such as cameras and sensors to operate, further reinforcing the efficacy of our proposals.

Alternatively, simulations of the proposed coordination network were completed in COOJA. The obtained results suggest the network can suitably support the communication requirements for a real-world deployment of the surveillance system. The results identify a difference in acknowledgement times across the collective UAV group, highlighting potential future areas of improvement.

Finally, a comprehensive assessment of the tracking capabilities of the group with appropriate networking delays modelled commenced. The results collected from this experiment confirm that the proposed communication network, with the small delays it adds, can effectively coordinate the multi-agent UAV group with negligible effect on its tracking accuracies.

These experiments confirmed the efficacy and feasibility of the proposed pipeline surveillance technique and the accompanying coordination network. Therefore, this research made a significant contribution to the literature, as a suitable coordination network for leader–follower structured multi-agent UAV groups was proposed and thoroughly evaluated. Additionally, this research also contributed to innovating existing pipeline surveillance techniques through the integration of previous multi-agent UAV advancements and networking.

Future work could address the evaluation of the performance of this system in a physical environment using multiple homogeneous UAVs. Our results suggest the system will perform accurately in real-world deployments; however, rigorous field testing is required to further validate these findings. To extend the simulation work, future steps should include simulating the UAV models in environments with physical disturbances like modelled wind. This would necessitate the derivation of potential collective disturbance rejection systems or inter-UAV collision avoidance systems to further the generalisability and reliability of our proposals.

Alternatively, further optimisation of the proposed coordination network could also be addressed in the future. This would involve real-world assessments of the network's communication outside of this study's COOJA environment. Additionally, investigating the fault tolerancy of the overall network is also something to consider. UAV nodes cannot always expect to be able to communicate with each other, so effective methods must be proposed to ensure that mission performance is not degraded in situations were communication pathways are lost. For future real-world deployments, especially in highly secure environments, the security of the proposed coordination network must also be addressed.

Author Contributions: Conceptualization, J.D., P.S.G., G.A. and M.I.; methodology, J.D., P.S.G., M.I. and E.S.; software, J.D. and P.S.G.; writing—original draft preparation, J.D., P.S.G. and G.A.; writing—review and editing, J.D., P.S.G. and M.I.; supervision, M.I. and E.S.; project administration, M.I. and E.S. All authors have read and agreed to the published version of the manuscript.

Funding: This research received no external funding. The APC was waived by the journal.

Institutional Review Board Statement: Not applicable.

Informed Consent Statement: Not applicable.

Data Availability Statement: The raw data supporting the conclusions of this article will be made available by the authors on request.

Conflicts of Interest: The authors declare no conflicts of interest.

References

1. Abdelkader, M.; Güler, S.; Jaleel, H.; Shamma, J.S. Aerial swarms: Recent applications and challenges. *Curr. Robot. Rep.* **2021**, *2*, 309–320. [CrossRef] [PubMed]
2. Radoglou-Grammatikis, P.; Sarigiannidis, P.; Lagkas, T.; Moscholios, I. A compilation of UAV applications for precision agriculture. *Comput. Netw.* **2020**, *172*, 107148. [CrossRef]
3. Nex, F.; Remondino, F. UAV for 3D mapping applications: A review. *Appl. Geomat.* **2014**, *6*, 1–15. [CrossRef]
4. Drummond, C.D.; Harley, M.D.; Turner, I.L.; Matheen, A.N.A.; Glamore, W.C. UAV applications to coastal engineering. In Proceedings of the Australasian Coasts & Ports Conference, Auckland, New Zealand, 15–18 September 2015; Volume 2015, p. 22nd.
5. Erdelj, M.; Natalizio, E. UAV-assisted disaster management: Applications and open issues. In Proceedings of the 2016 International Conference on Computing, Networking and Communications (ICNC), Kauai, HI, USA, 15–18 February 2016; pp. 1–5.
6. Mohsan, S.A.H.; Othman, N.Q.H.; Khan, M.A.; Amjad, H.; Żywiołek, J. A Comprehensive Review of Micro UAV Charging Techniques. *Micromachines* **2022**, *13*, 977. [CrossRef] [PubMed]
7. Islam, A.; Young Shin, S. A blockchain-based secure healthcare scheme with the assistance of unmanned aerial vehicle in Internet of Things. *Comput. Electr. Eng.* **2020**, *84*, 106627. [CrossRef]
8. Wang, P.; Luo, X.; Zhou, Z.; Zang, Y.; Hu, L. Key technology for Remote Sensing Information acquisitionbased on Micro UAV. *Trans. Chin. Soc. Agric. Eng.* **2014**, *30*, 1–12.
9. Cui, Q.; Liu, P.; Wang, J.; Yu, J. Brief analysis of drone swarms communication. In Proceedings of the 2017 IEEE International Conference on Unmanned Systems (ICUS), Beijing, China, 27–29 October 2017; pp. 463–466. [CrossRef]
10. Shrit, O.; Martin, S.; Alagha, K.; Pujolle, G. A new approach to realize drone swarm using ad-hoc network. In Proceedings of the 2017 16th Annual Mediterranean Ad Hoc Networking Workshop (Med-Hoc-Net), Budva, Montenegro, 28–30 June 2017; pp. 1–5. [CrossRef]
11. Cui, Y.; Jia, Y.; Li, Y.; Shen, J.; Huang, T.; Gong, X. Byzantine resilient joint localization and target tracking of multi-vehicle systems. *IEEE Trans. Intell. Veh.* **2023**, *8*, 2899–2913. [CrossRef]
12. Cui, Y.; Liang, Y.; Luo, Q.; Shu, Z.; Huang, T. Resilient Consensus Control of Heterogeneous Multi-UAV Systems with Leader of Unknown Input Against Byzantine Attacks. *IEEE Trans. Autom. Sci. Eng.* **2024**. [CrossRef]
13. Campion, M.; Ranganathan, P.; Faruque, S. A review and future directions of UAV swarm communication architectures. In Proceedings of the 2018 IEEE International Conference on Electro/Information Technology (EIT), Rochester, MI, USA, 3–5 May 2018; pp. 903–908.
14. Colefax, A.P.; Butcher, P.A.; Kelaher, B.P. The potential for unmanned aerial vehicles (UAVs) to conduct marine fauna surveys in place of manned aircraft. *ICES J. Mar. Sci.* **2017**, *75*, 1–8. [CrossRef]
15. Yan, C.; Xiang, X.; Wang, C.; Li, F.; Wang, X.; Xu, X.; Shen, L. PASCAL: Population-specific curriculum-based MADRL for collision-free flocking with large-scale fixed-wing UAV swarms. *Aerosp. Sci. Technol.* **2023**, *133*, 108091. [CrossRef]
16. Chen, H.; He, M.; Liu, J.; Xu, P.; Cao, X.; Han, W.; Yuan, G. A novel fractional-order flocking algorithm for large-scale UAV swarms. *Complex Intell. Syst.* **2023**, *9*, 6831–6844. [CrossRef]
17. Choutri, K.; Lagha, M.; Dala, L.; Lipatov, M. Quadrotors UAVs Swarming Control Under Leader-Followers Formation. In Proceedings of the 2018 22nd International Conference on System Theory, Control and Computing (ICSTCC), Sinaia, Romania, 10–12 October 2018; pp. 794–799. [CrossRef]
18. Lee, K.U.; Choi, Y.H.; Park, J.B. Backstepping Based Formation Control of Quadrotors with the State Transformation Technique. *Appl. Sci.* **2017**, *7*, 1170. [CrossRef]
19. Liang, Y.; Qi, D.; Yanjie, Z. Adaptive leader–follower formation control for swarms of unmanned aerial vehicles with motion constraints and unknown disturbances. *Chin. J. Aeronaut.* **2020**, *33*, 2972–2988. [CrossRef]
20. Nath, P.B.; Uddin, M.M. Tcp-ip model in data communication and networking. *Am. J. Eng. Res.* **2015**, *4*, 102–107.
21. Le Boudec, J.Y. The Transport Layer: TCP and UDP 2007. Available online: https://perso.ens-lyon.fr/eric.fleury/CPS/ASR2/slides/L3_ASR2_13_net_tcp.pdf (accessed on 1 August 2024).
22. Tsaoussidis, V.; Matta, I. Open issues on TCP for mobile computing. *Wirel. Commun. Mob. Comput.* **2002**, *2*, 3–20.
23. Fielding, R.; Gettys, J.; Mogul, J.; Frystyk, H.; Masinter, L.; Leach, P.; Berners-Lee, T. Hypertext Transfer Protocol–HTTP/1.1. Technical Report. 1999. Available online: https://www.w3.org/Protocols/rfc2616/rfc2616.html (accessed on 1 August 2024).
24. Vinoski, S. Advanced message queuing protocol. *IEEE Internet Comput.* **2006**, *10*, 87–89. [CrossRef]
25. Dobbelaere, P.; Esmaili, K.S. Kafka versus RabbitMQ: A comparative study of two industry reference publish/subscribe implementations: Industry Paper. In Proceedings of the 11th ACM International Conference on Distributed and Event-Based Systems, Barcelona, Spain, 19–23 June 2017; pp. 227–238.

26. Frodigh, M.; Johansson, P.; Larsson, P. Wireless ad hoc networking: The art of networking without a network. *Ericsson Rev.* **2000**, *4*, 249.
27. Khan, M.A.; Safi, A.; Qureshi, I.M.; Khan, I.U. Flying ad-hoc networks (FANETs): A review of communication architectures, and routing protocols. In Proceedings of the 2017 First International Conference on Latest Trends in Electrical Engineering and Computing Technologies (INTELLECT), Karachi, Pakistan, 15–16 November 2017; pp. 1–9. [CrossRef]
28. Johnson, D.B.; Maltz, D.A. Dynamic source routing in ad hoc wireless networks. In *Mobile Computing*; Springer: Boston, MA, USA, 1996; pp. 153–181.
29. Chelouah, L.; Semchedine, F.; Bouallouche-Medjkoune, L. Localization protocols for mobile wireless sensor networks: A survey. *Comput. Electr. Eng.* **2018**, *71*, 733–751. [CrossRef]
30. Coramik, M.; Ege, Y. Discontinuity inspection in pipelines: A comparison review. *Measurement* **2017**, *111*, 359–373. [CrossRef]
31. Clarke, E.S.; Krzewinski, T.G.; Metz, M.C. The Trans-Alaska Pipeline System Synthetically Insulated Workpad—An Evaluation of Present Conditions. *J. Energy Resour. Technol.* **1983**, *105*, 230–235. [CrossRef]
32. Company, A.P.S. *FACTS—Trans Alaska Pipeline System*; Alyeska Pipeline Service Company: Anchorage, AK, USA, 2021.
33. Hall, W.J.; Nyman, D.J.; Johnson, E.R.; Norton, J.D. Performance of the Trans-Alaska pipeline in the November 3, 2002 Denali fault earthquake. In *Advancing Mitigation Technologies and Disaster Response for Lifeline Systems*; American Society of Civil Engineers: Reston, VA, USA, 2003; pp. 522–534.
34. Alyeska Pipeline Service Company. Drones on TAPS. 2021. Available online: https://www.alyeska-pipe.com/pipeline_facts/drones-on-taps/ (accessed on 18 July 2023).
35. Society, R.A. BVLOS Drone Inspects Trans-Alaska Pipeline. 2019. Available online: https://www.aerosociety.com/news/bvlos-drone-inspects-trans-alaska-pipeline/ (accessed on 1 August 2024).
36. Chen, W.; Liu, J.; Guo, H.; Kato, N. Toward robust and intelligent drone swarm: Challenges and future directions. *IEEE Netw.* **2020**, *34*, 278–283. [CrossRef]
37. Asaamoning, G.; Mendes, P.; RosÃ¡rio, D.; Cerqueira, E. Drone Swarms as Networked Control Systems by Integration of Networking and Computing. *Sensors* **2021**, *21*, 2642. [CrossRef]
38. Yu, C.; Yang, Y.; Cheng, Y.; Wang, Z.; Shi, M.; Yao, Z. UAV-based pipeline inspection system with Swin Transformer for the EAST. *Fusion Eng. Des.* **2022**, *184*, 113277. [CrossRef]
39. Fernando, M.; Liu, L. Formation control and navigation of a quadrotor swarm. In Proceedings of the 2019 International Conference on Unmanned Aircraft Systems (ICUAS), Atlanta, GA, USA, 11–14 June 2019; pp. 284–291.
40. Cai, X.; Zhu, X.; Yao, W. Distributed adaptive time-varying formation of multi-UAV systems under undirected graph. *IET Intell. Transp. Syst.* **2024**, *18*, 218–229. [CrossRef]
41. Shao, S.; Peng, Y.; He, C.; Du, Y. Efficient path planning for UAV formation via comprehensively improved particle swarm optimization. *ISA Trans.* **2020**, *97*, 415–430. [CrossRef]
42. He, L.; Bai, P.; Liang, X.; Zhang, J.; Wang, W. Feedback formation control of UAV swarm with multiple implicit leaders. *Aerosp. Sci. Technol.* **2018**, *72*, 327–334. [CrossRef]
43. Hou, Y.; Zhao, J.; Zhang, R.; Cheng, X.; Yang, L. UAV swarm cooperative target search: A multi-agent reinforcement learning approach. *IEEE Trans. Intell. Veh.* **2023**, *9*, 568–578. [CrossRef]
44. Wang, Y.; Cao, J.; Kashkynbayev, A. Multi-agent bifurcation consensus-based multi-layer UAVs formation keeping control and its visual simulation. *IEEE Trans. Circuits Syst. Regul. Pap.* **2023**, *70*, 3221–3233. [CrossRef]
45. Morar, I.R.; Nascu, I. Model simplification of an unmanned aerial vehicle. In Proceedings of the 2012 IEEE International Conference on Automation, Quality and Testing, Robotics, Cluj-Napoca, Romania, 24–27 May 2012; pp. 591–596. [CrossRef]
46. Najm, A.A.; Ibraheem, I.K. Nonlinear PID controller design for a 6-DOF UAV quadrotor system. *Eng. Sci. Technol. Int. J.* **2019**, *22*, 1087–1097. [CrossRef]
47. Herrera, M.; Chamorro, W.; GÃ³mez, A.P.; Camacho, O. Sliding Mode Control: An Approach to Control a Quadrotor. In Proceedings of the 2015 Asia-Pacific Conference on Computer Aided System Engineering, Quito, Ecuador, 14–16 July 2015; pp. 314–319. [CrossRef]
48. Idrissi, M.; Salami, M.; Annaz, F. Modelling, simulation and control of a novel structure varying quadrotor. *Aerosp. Sci. Technol.* **2021**, *119*, 107093. [CrossRef]
49. Idrissi, M.; Annaz, F. Dynamic Modelling and Analysis of a Quadrotor Based on Selected Physical Parameters. *Int. J. Mech. Eng. Robot. Res.* **2020**, *9*, 784–790. [CrossRef]
50. Khatoon, S.; Shahid, M.; Ibraheem; Chaudhary, H. Dynamic modeling and stabilization of quadrotor using PID controller. In Proceedings of the 2014 International Conference on Advances in Computing, Communications and Informatics (ICACCI), Delhi, India, 24–27 September 2014; pp. 746–750. [CrossRef]
51. Salih, A.L.; Moghavvemi, M.; Mohamed, H.A.F.; Gaeid, K.S. Modelling and PID controller design for a quadrotor unmanned air vehicle. In Proceedings of the 2010 IEEE International Conference on Automation, Quality and Testing, Robotics (AQTR), Cluj-Napoca, Romania, 28–30 May 2010; Volume 1, pp. 1–5. [CrossRef]
52. Nagaty, A.; Saeedi, S.; Thibault, C.; Seto, M.; Li, H. Control and Navigation Framework for Quadrotor Helicopters. *J. Intell. Robot. Syst.* **2013**, *70*, 1–12. [CrossRef]
53. Pughat, A.; Bansal, B.; Verma, T. Performance Evaluation of Ad-Hoc Networks in Static & Mobile Environment. In Proceedings of the 2020 6th International Conference on Signal Processing and Communication (ICSC), Noida, India, 5–7 March 2020; pp. 51–57.

54. Laaouafy, M.; Lakrami, F.; Labouidya, O.; Elkamoun, N.; Iqdour, R. Comparative study of localization methods in WSN using Cooja simulator. In Proceedings of the 2019 7th Mediterranean Congress of Telecommunications (CMT), Fez, Morocco, 24–25 October 2019; pp. 1–5.
55. Al Qurashi, M.; Angelopoulos, C.M.; Katos, V. An architecture for resilient intrusion detection in ad-hoc networks. *J. Inf. Secur. Appl.* **2020**, *53*, 102530. [CrossRef]
56. Naik, K.P.; Joshi, U.R. Performance analysis of constrained application protocol using Cooja simulator in Contiki OS. In Proceedings of the 2017 International Conference on Intelligent Computing, Instrumentation and Control Technologies (ICICICT), Kerala, India, 6–7 July 2017; pp. 547–550. [CrossRef]
57. Frequently Asked Questions (FAQs) for Cisco Packet Tracer. Available online: https://www.netacad.com/courses/packet-tracer/faq#01 (accessed on 13 September 2023).
58. Jevtić, M.; Zogović, N.; Dimić, G. Evaluation of wireless sensor network simulators. In Proceedings of the 17th Telecommunications Forum (TELFOR 2009), Belgrade, Serbia, 24–26 November 2009; pp. 1303–1306.
59. Namboodiri, V.; Agarwal, M.; Gao, L. A study on the feasibility of mobile gateways for vehicular ad-hoc networks. In Proceedings of the 1st ACM International Workshop on Vehicular Ad Hoc Networks, Philadelphia, PA, USA, 1 October 2004; pp. 66–75.
60. Yu, S.; Fan, X.; Qi, J.; Wan, L.; Liu, B. Attitude control of quadrotor UAV based on integral backstepping active disturbance rejection control. *Trans. Inst. Meas. Control.* **2024**, *46*, 703–715. [CrossRef]
61. Le, W.; Xie, P.; Chen, J. Disturbance rejection control of the agricultural quadrotor based on adaptive neural network. *Inf. Process. Agric.* **2024**. [CrossRef]
62. Hendrawan, I.N.R.; Arsa, I.G.N.W. Zolertia Z1 energy usage simulation with Cooja simulator. In Proceedings of the 2017 1st International Conference on Informatics and Computational Sciences (ICICoS), Semarang, Indonesia, 15–16 November 2017; pp. 147–152. [CrossRef]
63. Morel, A.E.; Kavzak Ufuktepe, D.; Ignatowicz, R.; Riddle, A.; Qu, C.; Calyam, P.; Palaniappan, K. Enhancing Network-edge Connectivity and Computation Security in Drone Video Analytics. In Proceedings of the 2020 IEEE Applied Imagery Pattern Recognition Workshop (AIPR), Washington, DC, USA, 13–15 October 2020; pp. 1–12. [CrossRef]